Triple diffusive magneto convection in a fluid-porous composite system

Sumithra R.[1], Komala B.[2], Manjunatha N.[3]

[1]*Department of UG, PG Studies & Research in Mathematics,*
Nrupathunga University, Bengaluru, Karnataka, India
[2]*Department of Science and Humanities, PES University, Bengaluru, Karnataka, India*
[3]*Department of Mathematics, School of Applied Sciences, REVA University,*
Bengaluru, Karnataka, India

A study on triple diffusive magneto convection is made for a fluid – porous composite system with rigid-rigid boundaries insulated to temperature and concentration. The porous layer of the composite system is modeled using Darcy–Brinkman model. The method of regular perturbation approach is employed to find the eigen-value for the problem considered. The critical Rayleigh number as criterion for the onset of convection is derived for step function, salting below and desalting above salinity profiles. The effect of various physical parameter on the onset of convection is graphically depicted and the stability of the system is analyzed.

1. Introduction

The existence of convective instability in classical Benard problem, is determined by the temperature gradient between the top and bottom boundaries of the composite system. This instability due to diffusion heat alone is classified as single component convection. When the convection is caused by two opposing density components like heat and mass then the convection refers to double diffusive convection. When the convection is brought about by three different diffusivities (heat and two salts), it is referred as triple diffusive convection. The problems with three component convection is at high interest of many researchers as the occurrence of three diffusive component is quiet common and natural in almost all real time problems. It has enormous applications including fields of crystal growth, material processing, spacecraft, underground spread of chemical contaminants, petroleum reservoirs, waste disperse and fertilizer migration in saturated soil, alloy solidification and many more. The physical configuration with rigid-rigid boundaries are more suitable especially in the process of material processing. Astrophysical and geophysical applications triggered the investigation of magneto-convection in an electrically conducting horizontal fluid layer.

Oceanographers, astrophysicists, geophysicists, engineers and many others have increasingly been drawn attention to the study of convection in the application of an applied magnetic field [1, 2]. Thompson [3] and Chandrasekhar [4] were the first to examine magneto-convection in a horizontal fluid layer. Lortz [5] investigated magnetic field effects on double-diffusive convection. Rudraiah [6] studied in a Boussinesq fluid, the interaction of double-diffusive convection and an externally imposed vertical magnetic field. Siddheshwar and Pranesh [7] studied that in an electrically conducting Boussinesq fluid with suspended particles confined between an upper free/adiabatic and a lower rigid/isothermal boundary in a horizontal layer, the role of magnetic field in the inhibition of natural convection driven by combination of buoyancy and surface tension forces.

Jyoti Prakash et al. [8] have used the Darcy–Brinkman–Maxwell model to analyze the onset of convective instability in a triply diffusive Maxwell fluid saturated porous layer. They have established a sufficient condition for the validity of the principle exchange of stabilities and also the bounds for the complex growth rate were found with the conclusions that for the very general existence of the bounding surfaces, the results are universally true. Shivakumara and Naveen Kumar [9], analyzed the impact of couple stresses on linear and weakly nonlinear stability of a triply diffusive fluid layer using a modified perturbation technique. They have also measured heat and mass transfer based on the Nusselt number and discussed the influence of various physical parameters in detail. Manjunatha and Sumithra [10] have investigated triple diffusive magneto-convection in a composite system for three temperature profiles. Mukesh Kumar Awasthi et al. [11], analyzed a Maxwell fluid saturated porous layer for the onset of triple diffusive convection subjecting to a linear stability study in the presence of an internal heat source, and it was discovered that Lewis number has a destabiliing effect and solute Rayleigh number has a stabilizing effect. In a two-component system, the onset of double diffusive magneto-Marangoni convection have been investigated for non-uniform salinity gradients by Komala and Sumithra [12].

The work quoted above clarifies that numerous studies on magneto-convection in single fluid/porous layer and double-diffusive magneto-convection and triple-diffusive magneto-convection have been made. But, the occurrence of non uniform salinity gradients is the reality which is rarely touched. This work is an attempt to investigate the effect of non-uniform salinity gradients on triple diffusive natural convection in the existence of an applied magnetic field in a composite system.

2. Formulation of the problem

The triple diffusive magneto convection in composite system as shown in Fig. 1 is considered with rigid boundaries. The top and bottom boundaries are maintained at constant temperature and concentration differences. The rectangular coordinate system's origin is defined at the interface of fluid – porous composite system and the magnetic field is imposed along z-axis upwards. The Darcy–Brinkman model predicts that at the interface, the velocity, shear stress, normal stress, heat, heat flux, mass, and mass flux are all continuous. The governing equations are considered with Boussinesq approximation.

The governing equations for fluid layer (region-1) are, the laws of conservation of mass is

$$\nabla \cdot \boldsymbol{q} = 0;$$

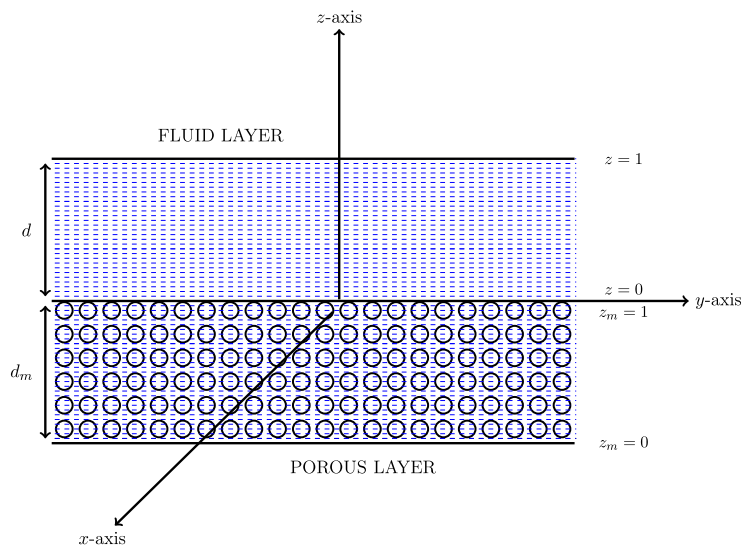the solenoidal property of magnetic field is

Fig. 1. Physical system.

$$\nabla \cdot \boldsymbol{H} = 0;$$

the momentum equation is

$$\rho_0 \left[\frac{\partial \boldsymbol{q}}{\partial t} + (\boldsymbol{q} \cdot \nabla) \boldsymbol{q} \right] = -\nabla P + \mu \nabla^2 \boldsymbol{q} - \rho g \hat{k} + \mu_p (\boldsymbol{H} \cdot \nabla) \boldsymbol{H};$$

the heat equation is

$$\frac{\partial T}{\partial t} + (\boldsymbol{q} \cdot \nabla) T = \kappa \nabla^2 T;$$

the concentration equations are

$$\frac{\partial C_1}{\partial t} + (\boldsymbol{q} \cdot \nabla) C_1 = \kappa_1 \nabla^2 C_1,$$

$$\frac{\partial C_2}{\partial t} + (\boldsymbol{q} \cdot \nabla) C_2 = \kappa_2 \nabla^2 C_2;$$

the equation for magnetic induction is

$$\frac{\partial \boldsymbol{H}}{\partial t} = \nabla \times \boldsymbol{q} \times \boldsymbol{H} + \nu \nabla^2 \boldsymbol{H};$$

the equation of state is

$$\rho = \rho_0 \left[1 - \alpha_t (T - T_0) + \alpha_{s1} (C_1 - C_0) + \alpha_{s2} (C_2 - C_0) \right].$$

The governing equations for porous layer (region-2),
the laws of conservation of mass is

$$\nabla_m \cdot \boldsymbol{q}_m = 0;$$

the solenoidal property of magnetic field is

$$\nabla_m \cdot \boldsymbol{H}_m = 0;$$

the Darcy–Brinkman equation for porous layer is

$$\rho_0 \left[\frac{1}{\varepsilon} \frac{\partial \boldsymbol{q}_m}{\partial t} + \frac{1}{\varepsilon^2} (\boldsymbol{q}_m \cdot \nabla_m) \boldsymbol{q}_m \right] = -\nabla_m P_m + \mu \nabla^2 \boldsymbol{q}_m - \frac{\mu}{K} \boldsymbol{q}_m - \rho_m g \hat{k}$$
$$+ \mu_p (\boldsymbol{H} \cdot \nabla_m) \boldsymbol{H} + \frac{q_m}{\sqrt{K}} c_b |\boldsymbol{q}_m| \boldsymbol{q}_m;$$

the heat equation is

$$A \frac{\partial T_m}{\partial t} + (\boldsymbol{q}_m \cdot \nabla_m) T_m = \kappa_m \nabla_m^2 T_m;$$

the concentration equations are

$$\phi \frac{\partial C_{m1}}{\partial t} + (\boldsymbol{q}_m \cdot \nabla_m) C_{m1} = \kappa_{m1} \nabla_m^2 C_{m1},$$

$$\phi \frac{\partial C_{m2}}{\partial t} + (\boldsymbol{q}_m \cdot \nabla_m) C_{m2} = \kappa_{m2} \nabla_m^2 C_{m2};$$

the magnetic induction equation is

$$\phi \frac{\partial \boldsymbol{H}_m}{\partial t} = \nabla_m \times \boldsymbol{q}_m \times \boldsymbol{H}_m + \nu_m \nabla_m^2 \boldsymbol{H}_m;$$

the equation of state is

$$\rho_m = \rho_0 \left[1 - \alpha_{tm} (T_m - T_0) + \alpha_{sm1} (C_{m1} - C_0) + \alpha_{sm2} (C_{m2} - C_0) \right],$$

where $\boldsymbol{q} = (u, v, w)$ is the velocity vector in fluid layer, ρ_0 is a reference density of the fluid, t is the time, $P = p + \frac{\mu_p H^2}{2}$ is the total pressure, μ is the dynamic viscosity, ρ is the density of the fluid, g is the gravity, T is the temperature, κ is the diffusivity of heat, C_1 and C_2 are the concentrations or the salinity fields, κ_1 is the solutal diffusivity of the first solute, κ_2 is the solutal diffusivity of the second solute, H is the magnetic field, ν is the effective magnetic viscosity, α_T is the thermal expansion co-efficient, α_{s1} and α_{s2} are the solute analog of α_T, ϕ is the porosity, K is the porous medium's permeability, μ_p is the effective viscosity of the porous medium, $A = \frac{(\rho_0 C_p)_m}{(\rho C_p)_f}$ is the heat capacities ratio, C_p is the specific heat. The quantities in porous medium are denoted by the subscript m.

The theoretical part of the study emphasizes upon using the process of regular perturbation to find solution to all above driving equations and attain the critical Rayleigh number for the salting below, desalting above and step function salinity gradients.

The solution is considered as below in equation (1) and (2), since the basic steady state is known to be at rest,

in the region-1,

$$[u, v, w, P, T, C_1, C_2, H] = [0, 0, 0, P_{bs}(z), T_{bs}(z), C_{bs1}(z), C_{bs2}(z), H_{bs}(z)], \tag{1}$$

and in region-2,

$$[u_m, v_m, w_m, P_m, T_m, C_{m1}, C_{m2}, H_m] = [0, 0, 0, P_{mbs}(z_m), T_{mbs}(z_m), C_{mbs1}(z_m), C_{mbs2}(z_m), H_{mbs}(z_m)]. \tag{2}$$

Infinitely small disruptions are implemented to focus on the stability of the basic steady state, in the region-1,

$$[\boldsymbol{q}, P, T, C_1, C_2, \boldsymbol{H}] = [0, P_{bs}(z), T_{bs}(z), C_{bs1}(z), C_{bs2}(z), H_{bs}(z)] + [\boldsymbol{q}', P', \theta, S_1, S_2, \boldsymbol{H}'],$$

and in region-2,

$$[\boldsymbol{q}_m, P_m, T_m, C_{m1}, C_{m2}, \boldsymbol{H}_m] = [0, P_{mbs}(z_m), T_{mbs}(z_m), C_{mbs1}(z_m), C_{mbs2}(z_m), H_{bs}(z_m)]$$
$$+ [\boldsymbol{q}'_m, P'_m, \theta_m, S_{m1}, S_{m2}, \boldsymbol{H}'],$$

where the perturbed counterparts are the primed quantities. The parameters are then non-dimensionalized with the use of d, $\frac{d^2}{\kappa}$, $\frac{\kappa}{d}$, $T_0 - T_u$, $C_{10} - C_{1u}$, $C_{20} - C_{2u}$, H_0 in the fluid layer as units of length, time, velocity, temperature, species concentrations, and magnetic field and d_m, $\frac{d_m^2}{\kappa_m}$, $\frac{\kappa_m}{d_m}$, $T_l - T_0$, $C_{1l} - C_{10}$, $C_{2l} - C_{20}$, H_{m0} as the porous layer's corresponding distinctive quantities. Two layers have different length scales, so each layer has the same depth. A detailed flow field is attained in both the layers of composite systems for all depth ratios $\hat{d} = \frac{d_m}{d}$. In the fluid and porous layers, solutions for dependent variables are obtained using normal mode analysis of the dimensionless equations for the perturbed variables. Supposing that the theory of exchange of instabilities remains true for composite layers, we obtain the following differential equations,
in $0 \leqslant z \leqslant 1$

$$\left(D^2 - a^2\right)^2 W = Ra^2\Theta - R_{s1}a^2\Sigma_1 - R_{s2}a^2\Sigma_2 + QD^2W, \tag{3}$$

$$\left(D^2 - a^2\right)\Theta + W = 0, \tag{4}$$

$$\tau_1\left(D^2 - a^2\right)\Sigma_1 + Wg(z) = 0, \tag{5}$$

$$\tau_2\left(D^2 - a^2\right)\Sigma_2 + W = 0; \tag{6}$$

in $0 \leqslant z_m \leqslant 1$

$$\left[(D_m^2 - a_m^2)\hat{\mu}\beta^2 - 1\right]\left(D_m^2 - a_m^2\right)W_m = R_m a_m^2\Theta_m - R_{sm1}a_m^2\Sigma_{m1}$$
$$- R_{sm2}a_m^2\Sigma_{m2} + Q_m\beta^2 D_m^2 W_m, \tag{7}$$

$$\left(D_m^2 - a_m^2\right)\Theta_m + W_m = 0, \tag{8}$$

$$\tau_{pm1}\left(D_m^2 - a_m^2\right)\Sigma_{m1} + W_m g_m(z_m) = 0, \tag{9}$$

$$\tau_{pm2}\left(D_m^2 - a_m^2\right)\Sigma_{m2} + W_m = 0. \tag{10}$$

The dimensionless numbers present in the above set of differential equations from (3) to (10) are, a is the horizontal wave number, W is the velocity, $R = \frac{g\alpha_T(T_0 - T_u)d^3}{\nu\kappa}$ is the Rayleigh number, $R_{sm1} = \frac{g\alpha_{S1}(C_{10} - C_{1u})d^3}{\nu\kappa}$ and $R_{sm2} = \frac{g\alpha_{S2}(C_{20} - C_{2u})d^3}{\nu\kappa}$ are the solute Rayleigh numbers, Θ is the temperature, Σ_1 and Σ_2 are the concentrations, $\tau_1 = \frac{\kappa_1}{\kappa}$ and $\tau_2 = \frac{\kappa_2}{\kappa}$ are diffusivity ratio, $Q = \frac{\mu_p H_0^2 d^2}{\mu\kappa\tau}$ is the Chandrashekara's number, $D = \frac{d}{dz}$, $h(z)$ is the salinity gradient with $\int_0^d h(z)dz = 1$ in region-1, $\hat{\mu} = \frac{\mu_p}{\mu}$ is the viscosity ratio, $\beta^2 = \frac{K}{d_p^2} = \text{Da}$ is the porous parameter and the suffix 'm' denotes dimensionless numbers in region-2.

3. Boundary conditions

At $z_m = d_m$, the boundary conditions are,

$$w_m = 0, \quad \frac{\partial w_m}{\partial z_m} = 0, \quad \frac{\partial \theta_m}{\partial z_m} = 0, \quad \frac{\partial S_{m1}}{\partial z_m} = 0, \quad \frac{\partial S_{m2}}{\partial z_m} = 0.$$

At $z = d$, the boundary conditions are,

$$w = 0, \quad \frac{\partial w}{\partial z} = 0, \quad \frac{\partial \theta}{\partial z} = 0, \quad \frac{\partial S_1}{\partial z} = 0, \quad \frac{\partial S_2}{\partial z} = 0.$$

At $z = 0$ and $z_m = 0$,

$$w = w_m, \quad \theta = \theta_m, \quad \frac{\partial w}{\partial z} = \frac{\partial w_m}{\partial z_m}, \quad \kappa \frac{\partial \theta}{\partial z} = \kappa_m \frac{\partial \theta_m}{\partial z_m},$$

$$S_1 = S_{m1}, \quad S_2 = S_{m2}, \quad D \frac{\partial S_1}{\partial z} = D_m \frac{\partial S_{m1}}{\partial z_m}, \quad D \frac{\partial S_2}{\partial z} = D_m \frac{\partial S_{m2}}{\partial z_m},$$

$$\hat{T} \tilde{d}^3 \beta^2 \left(3\nabla_2^2 + \frac{\partial^2}{\partial z^2} \right) \frac{\partial w}{\partial z} = -\frac{\partial w_m}{\partial z_m} + \hat{\mu} \beta^2 \left(3\nabla_{2m}^2 + \frac{\partial^2}{\partial z_m^2} \right) \frac{\partial w_m}{\partial z_m},$$

$$\left(-\frac{\partial^2 w}{\partial z^2} + \nabla_2^2 w \right) = \frac{\hat{\mu} \hat{T}}{\hat{d}} \left(-\frac{\partial^2 w_m}{\partial z_m^2} + \nabla_{2m}^2 w_m \right).$$

4. Solution by regular perturbation technique

Convection occurs at small range of horizontal wave number 'a', for both constant heat and mass flux boundaries, thus we expand

$$\begin{bmatrix} W \\ \Theta \\ \Sigma_1 \\ \Sigma_2 \end{bmatrix} = \sum_{j=0}^{\infty} a^{2j} \begin{bmatrix} W_j \\ \Theta_j \\ \Sigma_{j1} \\ \Sigma_{j2} \end{bmatrix}, \quad \begin{bmatrix} W_m \\ \Theta_m \\ \Sigma_{m1} \\ \Sigma_{m2} \end{bmatrix} = \sum_{j=0}^{\infty} a^{2j} \begin{bmatrix} W_{mj} \\ \Theta_{mj} \\ \Sigma_{mj1} \\ \Sigma_{mj2} \end{bmatrix}. \tag{11}$$

Using equation (11) in equations (3) to (10) we get the zero order differential equation in a^2 as in region-1,

$$D^4 W_0 - Q D^2 W_0 = 0, \tag{12}$$

$$D^2 \Theta_0 + W_0 = 0, \tag{13}$$

$$\tau_1 D^2 \Sigma_{10} + W_0 g(z) = 0, \tag{14}$$

$$\tau_2 D^2 \Sigma_{20} + W_{10} = 0; \tag{15}$$

and in region-2,

$$\hat{\mu} \beta^2 D_m^4 W_{m0} - D_m^2 W_{m0} - Q_m D_m^2 W_{m0} = 0, \tag{16}$$

$$D_m^2 \Theta_{m0} + W_{m0} = 0, \tag{17}$$

$$\tau_{m1} D_m^2 \Sigma_{m10} + W_{m0} g_m(z_m) = 0, \tag{18}$$

$$\tau_{m2} D_m^2 \Sigma_{m20} + W_{m10} = 0. \tag{19}$$

To solve above mentioned differential equations (12) to (19), the corresponding boundary conditions are as follows:

$$W_0(1) = 0, \quad DW_0(1) = 0, \quad D\Theta_0(1) = 0, \quad DS_{10}(1) = 0, \quad DS_{20}(1) = 0,$$

$$\hat{T} W_0(0) = W_{m0}(1), \quad \hat{T} \hat{d} DW_0(0) = D_m W_{m0}(1),$$

$$\hat{T} \tilde{d}^2 D^2 W_0(0) = \hat{\mu} D_m^2 W_{m0}(1), \quad D_m S_{m20}(0) = 0,$$

$$\Theta_0(0) = \hat{T} \Theta_{m0}(1), \quad D\Theta_0(0) = D_m \Theta_{m0}(1), \quad S_{10}(0) = \hat{S} S_{m10}(1),$$

$$DS_{10}(0) = D_m S_{m10}(1), \quad S_{20}(0) = \hat{S} S_{m20}(1), \quad DS_{20}(0) = D_m S_{m20}(1),$$
$$\hat{T}\hat{d}^3 \beta^2 D^3 W_0(0) = -D_m W_{m0}(1) + \hat{\mu}\beta^2 D_m^3 W_{m0}(1),$$
$$W_{m0}(0) = 0, \quad D_m W_{m0}(0) = 0, \quad D_m \Theta_{m0}(0) = 0, \quad D_m S_{m10}(0) = 0.$$

Zero order equations solution are given by,

$$W_0(z) = 0, \quad \Theta_0(z) = \hat{T}, \quad \Sigma_{10}(z) = \hat{S}_1, \quad \Sigma_{20}(z) = \hat{S}_2,$$
$$W_{m0}(z_m) = 0, \quad \Theta_{m0}(z_m) = 1, \quad \Sigma_{m10}(z_m) = 1, \quad \Sigma_{m20}(z_m) = 1.$$

The equations at the first order in a^2 are
for region-1,

$$D^4 W_1 - R\hat{T} + R_{s1}\hat{S}_1 + R_{s2}\hat{S}_2 - QD^2 W_1 = 0, \tag{20}$$

$$D^2 \Theta_1 - \hat{T} + W_1 = 0, \tag{21}$$

$$\tau_1 D^2 \Sigma_{11} - \tau_1 \hat{S}_1 + W_1 g(z) = 0, \tag{22}$$

$$\tau_2 D^2 \Sigma_{21} - \tau_2 \hat{S}_2 + W_1 = 0; \tag{23}$$

for region-2,

$$\hat{\mu}\beta^2 D_m^4 W_{m1} - D_m^2 W_{m1} - R_m + R_{sm1} + R_{sm2} - Q_m \beta^2 D_m^2 W_{m1} = 0, \tag{24}$$

$$D_m^2 \Theta_{m1} - 1 + W_{m1} = 0, \tag{25}$$

$$\tau_{m1} D_m^2 \Sigma_{m1} - \tau_{m1} + W_{m1} g_m(z_m) = 0, \tag{26}$$

$$\tau_{m2} D_m^2 \Sigma_{m2} - \tau_{m2} + W_{m1} = 0. \tag{27}$$

The following are the corresponding boundary conditions:

$$W_1(1) = 0, \quad DW_1(1) = 0, \quad D\Theta_1(1) = 0, \quad DS_1(1) = 0, \quad DS_2(1) = 0,$$
$$\hat{T}W_1(0) = \hat{d}^2 W_{m1}(1), \quad \hat{T}\hat{d}DW_1(0) = \hat{d}^2 D_m W_{m1}(1),$$
$$\hat{T}\hat{d}^2 D^2 W_1(0) = \hat{\mu} D_m^2 W_{m1}(1)\hat{d}^2, \quad S_1(0) = \hat{S}_1 \hat{d}^2 S_{m1}(1),$$
$$D_m S_{m2}(0) = 0, \quad \Theta_1(0) = \hat{T}\hat{d}^2 \Theta_{m1}(1), \quad D\Theta_1(0) = \hat{d}^2 D_m \Theta_{m1}(1),$$
$$DS_1(0) = \hat{d}^2 D_m S_{m1}(1), \quad S_2(0) = \hat{S}_1 \hat{d}^2 S_{m2}(1), \quad DS_2(0) = \hat{d}^2 D_m S_{m2}(1),$$
$$W_{m1}(0) = 0, \quad D_m W_{m1}(0) = 0, \quad D_m \Theta_{m1}(0) = 0, \quad D_m S_{m1}(0) = 0,$$
$$\hat{T}\hat{d}^3 \beta^2 D^3 W_1(0) = -\hat{d}^2 D_m W_{m1}(1) + \hat{\mu}\beta^2 \hat{d}^2 D_m^3 W_{m1}(1).$$

The solutions of Equations (20)–(23) and (24)–(27) give W_1 and W_{m1} as follows,

$$W_1(z) = C_1 + C_2 z + \cosh(\sqrt{Q}z)\left(C_3 + C_4 \tanh(\sqrt{Q}z)\right) - \frac{Az^2}{2Q}, \tag{28}$$

$$W_{m1}(z_m) = C_5 + C_6 z_m + \cosh\sqrt{p}z_m \left(C_7 + C_8 \tanh\sqrt{p}z_m\right) - B z_m{}^2, \tag{29}$$

where $p = \sqrt{\frac{1}{\hat{\mu}\beta^2}}$ and C_{i^s}, $i = 1$ to 8 are constants found using the velocity boundary conditions as below,

$$A = R\hat{T} - R_{s1}\hat{S}_1 - R_{s2}\hat{S}_2, \quad B = \frac{R_m - R_{sm1} - R_{sm2}}{2(1 + Q_m\beta^2)},$$

$$C_1 = \frac{A\delta_{29} + B\delta_{30}}{\hat{T}}, \quad C_2 = A\delta_{31} + B\delta_{32}, \quad C_3 = A\delta_{33} + B\delta_{34},$$

$$C_4 = A\delta_{35} + B\delta_{36}, \quad C_5 = -C_7, \quad C_6 = -\sqrt{p}C_8,$$

$$C_7 = A\delta_{27} + B\delta_{28}, \quad C_8 = A\delta_{25} + B\delta_{26}$$

$$\delta_1 = \hat{d}^2(\cosh\sqrt{p} - 1) - \frac{\hat{\mu}}{Q}p\cosh\sqrt{p}, \quad \delta_2 = \hat{d}^2(\sinh\sqrt{p} - \sqrt{p}) - \frac{\hat{\mu}}{Q}p\sinh\sqrt{p},$$

$$\delta_3 = \frac{-\delta_1}{\hat{T}} - \frac{\hat{\mu}}{Q\hat{T}}p\cosh\sqrt{Q}\cosh\sqrt{p}, \quad \delta_4 = \frac{-\delta_2}{\hat{T}} - \frac{\hat{\mu}}{Q\hat{T}}p\cosh\sqrt{Q}\sinh\sqrt{p},$$

$$\delta_5 = \left(\frac{1}{2} + \frac{1}{Q} - \frac{\cosh\sqrt{Q}}{Q}\right)\frac{1}{Q}, \quad \delta_6 = \left(\frac{\frac{\hat{\mu}}{Q} - \frac{\hat{d}^2}{2}}{\hat{T}} + \frac{\hat{\mu}\cosh\sqrt{Q}}{\hat{T}Q}\right)\frac{1}{1 + Q_m\beta^2},$$

$$\delta_7 = -\frac{\sqrt{Q}\hat{\mu}p}{Q\hat{T}}\cosh\sqrt{p}\sinh\sqrt{Q}, \quad \delta_8 = -\frac{\sqrt{Q}\hat{\mu}p}{Q\hat{T}}\sinh\sqrt{p}\sinh\sqrt{Q},$$

$$\delta_9 = \frac{1}{Q}\left(1 - \frac{\sqrt{Q}\sinh\sqrt{Q}}{Q}\right), \quad \delta_{10} = \frac{\hat{\mu}\sqrt{Q}\sinh\sqrt{Q}}{\hat{T}Q\left(1 + Q_m\beta^2\right)},$$

$$\delta_{11} = \frac{\delta_3 - \delta_7}{\sinh\sqrt{Q} - \sqrt{Q}\cosh\sqrt{Q}}, \quad \delta_{12} = \frac{\delta_4 - \delta_8}{\sinh\sqrt{Q} - \sqrt{Q}\cosh\sqrt{Q}},$$

$$\delta_{13} = \frac{\delta_5 - \delta_9}{\sinh\sqrt{Q} - \sqrt{Q}\cosh\sqrt{Q}}, \quad \delta_{37} = \frac{\delta_6 + \delta_{10}}{\sinh\sqrt{Q} - \sqrt{Q}\cosh\sqrt{Q}},$$

$$\delta_{14} = \frac{1}{\hat{T}\hat{d}\beta^2 Q\sqrt{Q}\left(1 + Q_m\beta^2\right)} + \delta_{37}, \quad \delta_{15} = -\sinh\sqrt{Q}\delta_{11} + \delta_3,$$

$$\delta_{16} = -\sinh\sqrt{Q}\delta_{12} + \delta_4, \quad \delta_{17} = -\sinh\sqrt{Q}\delta_{13} + \delta_5,$$

$$\delta_{18} = \sinh\sqrt{Q}\delta_{37} - \delta_6, \quad \delta_{19} = \hat{T}\delta_{15} + \hat{T}\sqrt{Q}\delta_{11} + \hat{d}\sqrt{p}\sinh\sqrt{p},$$

$$\delta_{20} = \hat{T}\delta_{16} + \hat{T}\sqrt{Q}\delta_{12} + \hat{d}\sqrt{p} - \hat{d}\sqrt{p}\cosh\sqrt{p}, \quad \delta_{21} = \hat{T}\delta_{17} + \hat{T}\sqrt{Q}\delta_{13},$$

$$\delta_{22} = \hat{T}\delta_{18} - \hat{T}\sqrt{Q}\delta_{37} + \frac{\hat{d}}{\left(1 + Q_m\beta^2\right)}, \quad \delta_{23} = \frac{\hat{\mu}\beta^2 p\sqrt{p}\sinh\sqrt{p} - \sqrt{p}\sinh\sqrt{p}}{\hat{T}\hat{d}\beta^2 Q\sqrt{Q}} - \delta_{11},$$

$$\delta_{24} = \frac{\sqrt{p} + \hat{\mu}\beta^2 p\sqrt{p}\cosh\sqrt{p} - \sqrt{p}\cosh\sqrt{p}}{\hat{T}\hat{d}\beta^2 Q\sqrt{Q}} - \delta_{12}, \quad \delta_{25} = \frac{\delta_{21}\delta_{23} + \delta_{13}\delta_{19}}{\delta_{19}\delta_{24} - \delta_{20}\delta_{23}},$$

$$\delta_{26} = \frac{\delta_{22}\delta_{23} - \delta_{14}\delta_{19}}{\delta_{19}\delta_{24} - \delta_{20}\delta_{23}}, \quad \delta_{27} = \frac{-\delta_{20}\delta_{25} - \delta_{21}}{\delta_{19}}, \quad \delta_{28} = \frac{-\delta_{20}\delta_{26} - \delta_{22}}{\delta_{19}},$$

$$\delta_{29} = \delta_1\delta_{27} + \delta_2\delta_{25} - \frac{\hat{T}}{Q^2}, \quad \delta_{30} = \delta_1\delta_{28} + \delta_2\delta_{26} + \frac{2\hat{\mu} - Q\hat{d}^2}{2Q\left(1 + Q_m\beta^2\right)},$$

$$\delta_{31} = \delta_{27}\left(-\sinh\sqrt{Q}\delta_{11} + \delta_3\right) + \delta_{25}\delta_{38} - \sinh\sqrt{Q}\delta_{13} + \delta_5,$$

$$\delta_{32} = \delta_{28}\left(-\sinh\sqrt{Q}\delta_{11} + \delta_3\right) + \delta_{26}\delta_{38} + \sinh\sqrt{Q}\delta_{37} - \delta_6,$$

$$\delta_{33} = \frac{\hat{\mu}p\cosh\sqrt{p}}{\hat{T}Q}\delta_{27} + \frac{\hat{\mu}p\cosh\sqrt{p}}{\hat{T}Q}\delta_{25} + \frac{1}{Q^2}, \quad \delta_{38} = -\sinh\sqrt{Q}\delta_{12} + \delta_4,$$

$$\delta_{34} = \frac{\hat{\mu}p\cosh\sqrt{p}}{\hat{T}Q}\delta_{28} + \frac{\hat{\mu}p\sinh\sqrt{p}}{\hat{T}Q}\delta_{26} - \frac{\hat{\mu}}{\hat{T}Q\left(1 + Q_m\beta^2\right)},$$

$$\delta_{35} = \delta_{11}\delta_{27} + \delta_{12}\delta_{25} + \delta_{13}, \quad \delta_{36} = \delta_{11}\delta_{28} + \delta_{12}\delta_{26} - \delta_{37}.$$

4.1. The condition of solvability

The condition of solvability is obtained from the differential equation of temperature and concentration and using their respective boundary conditions as below,

$$\int_0^1 W_1 dz + \tau_{pm1}\int_0^1 W_1 g(z) dz + \hat{d}^2\int_0^1 W_{m1} dz_m + \tau_1\hat{d}^2\int_0^1 W_{m1} g_m(z_m) dz_m + \tau_{pm2}\int_0^1 W_1 dz$$

$$+ \tau_2\hat{d}^2\int_0^1 W_{m1} dz_m = \hat{T} + \hat{d}^2 + \tau_1\tau_{pm1}\left(\hat{S}_1 + \hat{d}^2\right) + \tau_2\tau_{pm2}\left(\hat{S}_2 + \hat{d}^2\right). \quad (30)$$

We compute the critical Rayleigh number R_c for step function, salting below and desalting above salinity profiles by substituting expressions for W_m and W_{m1} from equations (28) and (29) in equation (30).

4.2. Step function salinity profile

The basic composition gradually decreases in this salinity profile by ΔS at $z = \varepsilon$ and ΔS_m at $z_m = \varepsilon_m$ otherwise uniform. Accordingly,

$$g(z) = \delta(z - \varepsilon), \quad g_m(z_m) = \delta(z_m - \varepsilon_m).$$

The depth of saline in the fluid layer is ε whereas the depth of saline in the porous layer is ε_m. The condition of solvability (30) has been used to evaluate the critical Rayleigh number for this profile and as proceeds,

$$R_c = \frac{\Delta_1 + \left(R_{s1}\hat{S}_1 + R_{s2}\hat{S}_2\right)\Delta_{12} + \left(R_{sm1} + R_{sm2}\right)\Delta_{13}}{\hat{T}\left(\Delta_{12} + \frac{\hat{d}^3\beta^2\Delta_{13}}{\kappa}\right)},$$

where $\Delta_i'^s$ are given by

$$\Delta_1 = \hat{T} + \hat{d}^2 + \tau_1\,\tau_{pm1}\left(\hat{S} + \hat{d}^2\right) + \tau_2\,\tau_{pm2}\left(\hat{S}_2 + \hat{d}^2\right),$$

$$\Delta_2 = 1 + \tau_{pm1} + \tau_{pm2}, \quad \Delta_3 = \varepsilon\tau_{pm1} + \frac{1 + \tau_{pm2}}{2},$$

$$\Delta_4 = \tau_{pm1}\cosh\sqrt{Q}\varepsilon + \frac{(1 + \tau_{pm2})}{\sqrt{Q}}\sinh\sqrt{Q},$$

$$\Delta_5 = \tau_{pm1}\sinh\sqrt{Q}\varepsilon + \frac{(1 + \tau_{pm2})}{\sqrt{Q}}\left(\cosh\sqrt{Q} - 1\right),$$

$$\Delta_6 = \frac{\varepsilon^2\tau_{pm1}}{2Q} + \frac{(1 + \tau_{pm2})}{6Q}, \quad \Delta_7 = \hat{d}^2\left(1 + \tau_1 + \tau_2\right), \quad \Delta_8 = \hat{d}^2\left(\varepsilon_m\tau_1 + \frac{1 + \tau_2}{2}\right),$$

$$\Delta_9 = \hat{d}^2\left(\tau_1\cosh\sqrt{p}\varepsilon_m + \frac{(1 + \tau_2)}{\sqrt{p}}\sinh\sqrt{p}\right),$$

$$\Delta_{10} = \hat{d}^2\left(\tau_1\sinh\sqrt{p}\varepsilon_m + \frac{(1 + \tau_2)\left(\cosh\sqrt{p} - 1\right)}{\sqrt{p}}\right),$$

$$\Delta_{11} = \hat{d}^2\left(\frac{\tau_1\varepsilon_m^2}{2\left(1 + Q_m\beta^2\right)} + \frac{1 + \tau_2}{6(1 + Q_m\beta^2)}\right),$$

$$\Delta_{12} = \frac{\delta_{29}\Delta_2}{\hat{T}} + \delta_{31}\Delta_3 + \delta_{33}\Delta_4 + \delta_{35}\Delta_5 - \Delta_6 - \Delta_{121},$$

$$\Delta_{13} = \frac{\delta_{30}\Delta_2}{\hat{T}} + \delta_{32}\Delta_3 + \delta_{34}\Delta_4 + \delta_{36}\Delta_5 - \Delta_{11} - \Delta_{131},$$

$$\Delta_{121} = \delta_{27}\Delta_7 - \sqrt{p}\delta_{25}\Delta_8 + \delta_{27}\Delta_9 + \delta_{25}\Delta_{10},$$

$$\Delta_{131} = \delta_{28}\Delta_7 - \sqrt{p}\delta_{26}\Delta_8 + \delta_{28}\Delta_9 + \delta_{26}\Delta_{10}.$$

4.3. Piecewise linear salting from below salinity profile

For this considered profile following Currie [13], we assess

$$g(z) = \begin{cases} \varepsilon^{-1}, & 0 \leqslant z \leqslant \varepsilon, \\ 0, & \varepsilon \leqslant z \leqslant 1, \end{cases} \qquad g_m(z_m) = \begin{cases} \varepsilon_m^{-1}, & 0 \leqslant z_m \leqslant \varepsilon_m, \\ 0, & \varepsilon_m \leqslant z_m \leqslant 1. \end{cases}$$

The condition of solvability (30) has been used to evaluate the critical Rayleigh number for this profile and as proceeds,

$$R_c = \frac{\Delta_1 + \left(R_{s1}\hat{S}_1 + R_{s2}\hat{S}_2\right)\Delta_{12} + \left(R_{sm1} + R_{sm2}\right)\Delta_{13}}{\hat{T}\left(\Delta_{12} + \frac{\hat{d}^3\beta^2\Delta_{13}}{\kappa}\right)},$$

where $\Delta_i'^s$ are

$$\Delta_1 = \hat{T} + \hat{d}^2 + \tau_1\,\tau_{pm1}\left(\hat{S} + \hat{d}^2\right) + \tau_2\,\tau_{pm2}\left(\hat{S}_2 + \hat{d}^2\right),$$

$$\Delta_2 = 1 + \tau_{pm1} + \tau_{pm2}, \quad \Delta_3 = \frac{1}{2}\left(\varepsilon\tau_{pm1} + 1 + \tau_{pm2}\right),$$

$$\Delta_4 = \frac{\tau_{pm1}}{\varepsilon\sqrt{Q}}\sinh\sqrt{Q}\varepsilon + \frac{(1+\tau_{pm2})}{\sqrt{Q}}\sinh\sqrt{Q},$$

$$\Delta_5 = \frac{\tau_{pm1}}{\varepsilon\sqrt{Q}}(\cosh\sqrt{Q}\varepsilon - 1) + \frac{(1+\tau_{pm2})}{\sqrt{Q}}(\cosh\sqrt{Q} - 1),$$

$$\Delta_6 = \frac{\varepsilon^2\tau_{pm1}}{6Q} + \frac{(1+\tau_{pm2})}{6Q}, \quad \Delta_7 = \hat{d}^2(1+\tau_1+\tau_2),$$

$$\Delta_8 = \frac{\hat{d}^2}{2}(\varepsilon_m\tau_1 + 1 + \tau_2), \quad \Delta_9 = \frac{\hat{d}^2}{\sqrt{p}}\left(\frac{\tau_1\sinh\sqrt{p}\varepsilon_m}{\varepsilon_m} + \frac{(1+\tau_2)}{\sqrt{p}}\sinh\sqrt{p}\right),$$

$$\Delta_{10} = \frac{\hat{d}^2}{\sqrt{p}}\left(\frac{\tau_1(\cosh\sqrt{p}\varepsilon_m - 1)}{\varepsilon_m} + (1+\tau_2)(\cosh\sqrt{p} - 1)\right),$$

$$\Delta_{11} = \frac{\hat{d}^2}{6(1+Q_m\beta^2)}\left(\tau_1\varepsilon_m^2 + 1 + \tau_2\right),$$

$$\Delta_{12} = \frac{\delta_{29}\Delta_2}{\hat{T}} + \delta_{31}\Delta_3 + \delta_{33}\Delta_4 + \delta_{35}\Delta_5 - \Delta_6 - \Delta_{121},$$

$$\Delta_{13} = \frac{\delta_{30}\Delta_2}{\hat{T}} + \delta_{32}\Delta_3 + \delta_{34}\Delta_4 + \delta_{36}\Delta_5 - \Delta_{11} - \Delta_{131},$$

$$\Delta_{121} = \delta_{27}\Delta_7 - \sqrt{p}\delta_{25}\Delta_8 + \delta_{27}\Delta_9 + \delta_{25}\Delta_{10},$$

$$\Delta_{131} = \delta_{28}\Delta_7 - \sqrt{p}\delta_{26}\Delta_8 + \delta_{28}\Delta_9 + \delta_{26}\Delta_{10}.$$

4.4. Piecewise linear desalting above salinity profile

For desalting from above salinity profile following Vidal and Acrivos [14], we consider

$$g(z) = \begin{cases} 0, & 0 \leqslant z \leqslant (1-\varepsilon), \\ \varepsilon^{-1}, & (1-\varepsilon) \leqslant z \leqslant 1, \end{cases} \quad g_m(z_m) = \begin{cases} 0, & 0 \leqslant z_m \leqslant (1-\varepsilon_m), \\ \varepsilon_m^{-1}, & (1-\varepsilon_m) \leqslant z_m \leqslant 1. \end{cases}$$

The condition of solvability (30) has been used to evaluate the critical Rayleigh number for this profile and as proceeds,

$$R_c = \frac{\Delta_1 + \left(R_{s1}\hat{S}_1 + R_{s2}\hat{S}_2\right)\Delta_{12} + \left(R_{sm1} + R_{sm2}\right)\Delta_{13}}{\hat{T}\left(\Delta_{12} + \frac{\hat{d}^3\beta^2\Delta_{13}}{\kappa}\right)},$$

where $\Delta_i's$ are given by

$$\Delta_1 = \hat{T} + \hat{d}^2 + \tau_1\tau_{pm1}\left(\hat{S} + \hat{d}^2\right) + \tau_2\tau_{pm2}\left(\hat{S}_2 + \hat{d}^2\right),$$

$$\Delta_2 = 1 + \tau_{pm1} + \tau_{pm2}, \quad \Delta_3 = \frac{1}{2}\left(\frac{\tau_{pm1}}{\varepsilon}\left(1 - (1-\varepsilon)^2\right) + (1+\tau_{pm2})\right),$$

$$\Delta_4 = \frac{\tau_{pm1}}{\varepsilon\sqrt{Q}}\left(\sinh\sqrt{Q} - \sinh\sqrt{Q}(1-\varepsilon)\right) + \frac{(1+\tau_{pm2})}{\sqrt{Q}}\sinh\sqrt{Q},$$

$$\Delta_5 = \frac{\tau_{pm1}}{\varepsilon\sqrt{Q}}\left(\cosh\sqrt{Q} - \cosh\sqrt{Q}(1-\varepsilon)\right) + \frac{(1+\tau_{pm2})}{\sqrt{Q}}\left(\cosh\sqrt{Q} - 1\right),$$

$$\Delta_6 = \frac{\tau_{pm1}}{6Q\varepsilon}\left(1 - (1-\varepsilon)^3\right) + \frac{(1+\tau_{pm2})}{6Q}, \quad \Delta_7 = \hat{d}^2(1+\tau_1+\tau_2),$$

$$\Delta_8 = \frac{\hat{d}^2}{2}\left(\frac{\tau_1}{\varepsilon_m}\left(1 - (1-\varepsilon_m)^2\right) + (1+\tau_2)\right),$$

$$\Delta_9 = \frac{\hat{d}^2}{\sqrt{p}}\left(\frac{\tau_1}{\varepsilon_m}(\sinh\sqrt{p} - \sinh\sqrt{p}(1-\varepsilon_m)) + (1+\tau_2)\sinh\sqrt{p}\right),$$

$$\Delta_{10} = \frac{\hat{d}^2}{\sqrt{p}} \left(\frac{\tau_1}{\varepsilon_m}(\cosh \sqrt{p} - \cosh \sqrt{p}(1 - \varepsilon_m)) + (1 + \tau_2)(\cosh \sqrt{p} - 1) \right),$$

$$\Delta_{11} = \frac{\hat{d}^2}{6(1 + Q_m \beta^2)} \left(\frac{\tau_1(1 - (1 - \varepsilon_m)^3)}{\varepsilon_m} + (1 + \tau_2) \right),$$

$$\Delta_{12} = \frac{\delta_{29}\Delta_2}{\hat{T}} + \delta_{31}\Delta_3 + \delta_{33}\Delta_4 + \delta_{35}\Delta_5 - \Delta_6 - \Delta_{121},$$

$$\Delta_{13} = \frac{\delta_{30}\Delta_2}{\hat{T}} + \delta_{32}\Delta_3 + \delta_{34}\Delta_4 + \delta_{36}\Delta_5 - \Delta_{11} - \Delta_{131},$$

$$\Delta_{121} = \delta_{27}\Delta_7 - \sqrt{p}\delta_{25}\Delta_8 + \delta_{27}\Delta_9 + \delta_{25}\Delta_{10},$$

$$\Delta_{131} = \delta_{28}\Delta_7 - \sqrt{p}\delta_{26}\Delta_8 + \delta_{28}\Delta_9 + \delta_{26}\Delta_{10}.$$

5. Graphical interpretations

The graphs which are discussion in this section are plotted by considering critical Rayleigh number R_c along y-axis and saline depth ε along x-axis with $0 \leqslant \varepsilon \leqslant 1$ for step function, salting below and desalting above salinity profiles for triple diffusive magneto convection. The graphs are projected for known fixed set of values $\mathrm{Da} = 0.1$, $\kappa = 1$, $\hat{\mu} = 2.5$, $\tau_1 = \tau_2 = 0.25$, $\tau_{pm1} = \tau_{pm2} = 0.75$, $\hat{S}_1 = \hat{S}_2 = \hat{T} = 1$, $\hat{d} = 1$, $R_{s1} = R_{s2} = 5$ and $Q = 2$ for all the salinity profiles discussed in previous section.

The effect of step function, salting below and desalting above salinity profiles on the onset of magneto convection with three diffusive components is depicted in Figure 2. Table 1 infers that a suitable choice of salinity profile can be made in order to control the onset of convection in the composite system.
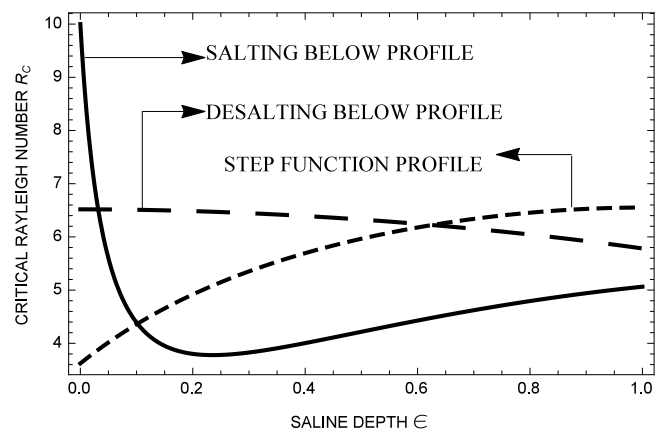
Fig. 2. Critical Rayleigh number R_c versus the saline depth ε.

Table 1.

Saline depth range	Stable profile	Unstable profile
$0 \leqslant \varepsilon \leqslant 0.05$	salting from below profile	step function profile
$0.05 \leqslant \varepsilon \leqslant 0.6$	desalting from above profile	salting from below profile
$0.6 \leqslant \varepsilon \leqslant 1$	step function profile	salting from below profile

Figure 3 depicts the influence of the Darcy number $\mathrm{Da} = \sqrt{\beta}$, which is the porous parameter in concern of critical Rayleigh number R_c for salting below, desalting above and step function profiles. Figure 3 indicates that critical Rayleigh number R_c increases as Darcy number Da enhances in all profiles for a fixed number of saline depth ε. This delays the onset of convection in the composite system. Thus the system is stabilized.

The effect of the porosity e, depicted graphically in Figure 4 for salting below, desalting above and step function profiles. Figure 4 indicates that critical Rayleigh number R_c decreases as porosity e enhances in all profiles for fixed number of saline depth ε. This accelerates the onset of convection in composite system. Thus the system is destabilized.

The effects of the magnetic field Q on R_c is graphically shown in Figure 5 for salting below, desalting above and step function profiles. From the graph, for fixed values of saline depth ε critical Rayleigh number R_c increases as Q enhances in all profiles. This delays the convection in the composite system. Thus the system is stabilized.
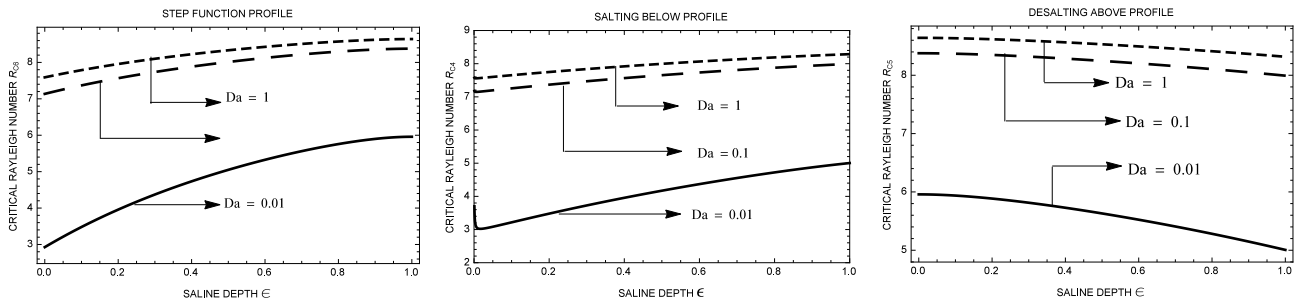
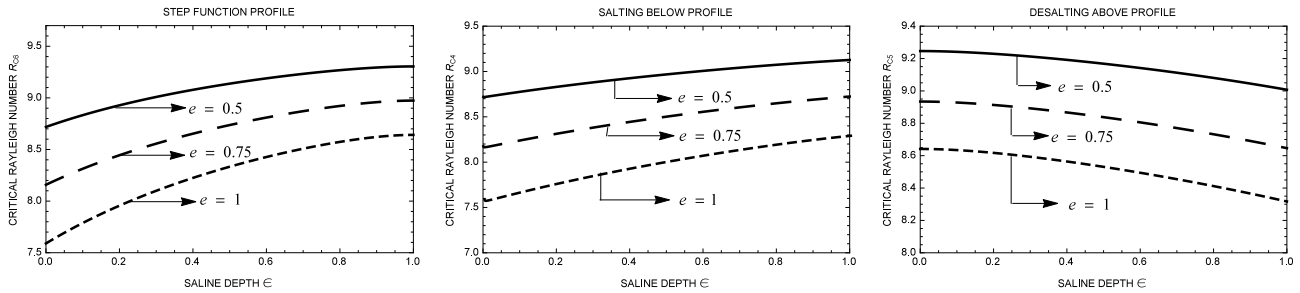**Fig. 3.** The effect of Darcy number $Da = 0.01, 0.1, 1$.

Fig. 4. The effect of porosity $e = 0.5, 0.75, 1$.
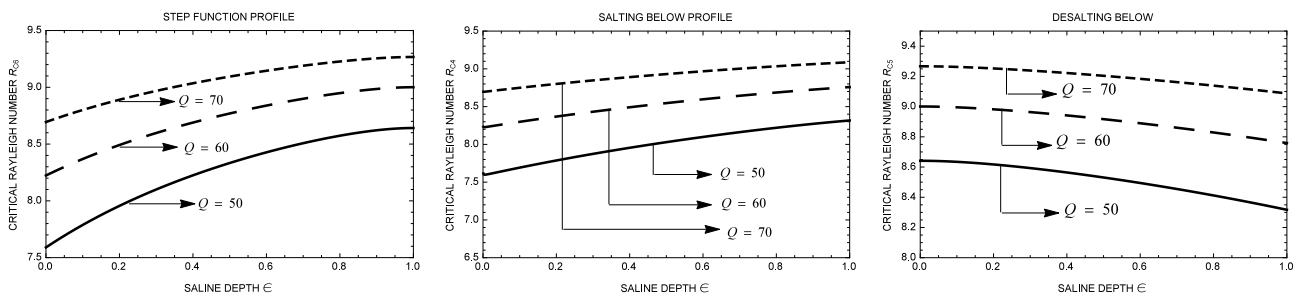

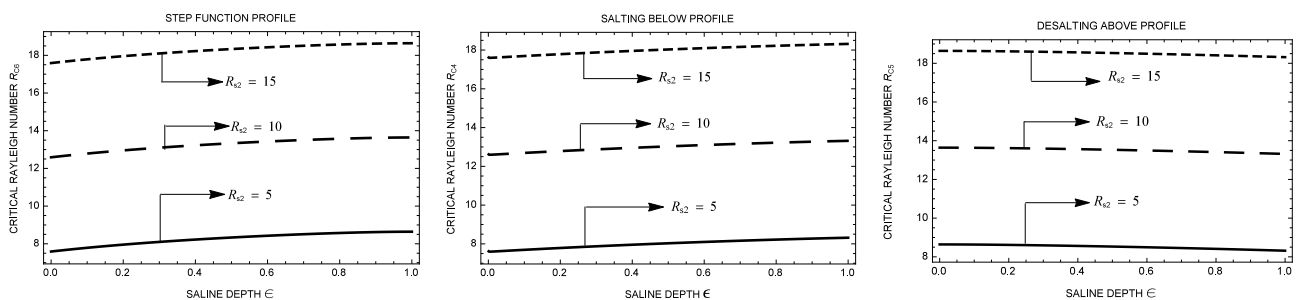**Fig. 5.** The effect of the magnetic field $Q = 50, 60, 70$.

Fig. 6. The effect of solute Rayleigh number $R_{s2} = 5, 10, 15$.

The influence of the solute Rayleigh number R_{s2} of the second solute is seen in Figure 6 for salting below, desalting above and step function profiles. From the curves in Figure 6, for a fixed number of saline depth ε, increasing the value of the solute Rayleigh number R_{s2} enhances the value of the critical Rayleigh number R_c. The onset of convection in the composite system is slowed as a result of this. Also as a consequence, the system has been stabilized.

6. Conclusions

The onset of triple diffusive magneto convection in the composite system is investigated using regular perturbation technique for the composite system with rigid–rigid boundaries. The graphs are projected

with critical Rayleigh number along y-axis and saline depth along the x-axis with the saline depth ε varying from 0 to 1. The influence of various physical parameters on the onset of triple diffusive magneto convection are shown graphically in Section 5.

1. With the increase in the value of the physical parameters solute Rayleigh number R_{s2}, Darcy number Da and Chandrashekara's number Q, the critical Rayleigh number R_c enhances in all the salinity profiles as observed from the graphs in Section 6, because of which the convection sets in slowly. Thus, these parameters stabilizes the composite system.

2. As a result of managing these parameters, stability-demanding conditions such as solar pond, crystal growth can be effectively managed.

3. The critical Rayleigh number R_c decreases with the increase in the value of porosity e of the porous layer in fluid-porous composite system for all the salinity profiles considered in Section 5. The convection sets in at a faster pace due to this decrease in critical Rayleigh number. Thus the porosity of the porous layer destabilizes the composite system.

4. In the process of manufacture of permanent magnetic material, the destabilizing effects under normal gravity conditions are more efficient. Thus, by increasing the porosity of the porous medium, a high-quality permanent magnetic material can be made.

[1] Turner J. S. Buoyancy Effects in Fluids. University of Cambridge (1979).

[2] Rudraiah N., Shivakumara I. S. Double-diffusive convection with an imposed magnetic field. International Journal of Heat and Mass Transfer. **27** (10), 1825–1836 (1984).

[3] Thompson W. B. Thermal convection in a magnetic field. Philosophical Magazine. **42** (335), 1417–1432 (1951).

[4] Chandrasekhar S. Hydrodynamic and Hydromagnetic Stability. Oxford University Press, London, UK (1961).

[5] Lortz D. A stability criterion for steady finite amplitude convection with an external magnetic field. Journal of Fluid Mechanics. **23** (1), 113–128 (1965).

[6] Rudraiah N. Double-diffusive magnetoconvection. Pramana. **27**, 233–266 (1986).

[7] Siddheshwar P. G., Pranesh S. Magnetoconvection in fluids with suspended particles under $1g$ and μg. Aerospace Science and Technology. **6** (2), 105–114 (2002).

[8] Prakash J., Kumari K., Kumar R. Triple diffusive convection in a Maxwell fluid saturated porous layer: Darcy–Brinkman–Maxwell Model. Journal of Porous Media. **19** (10), 87–883 (2016).

[9] Shivakumara I. S., Naveen Kumar S. B. Linear and weakly nonlinear triple diffusive convection in a couple stress fluid layer. International Journal of Heat and Mass Transfer. **68**, 542–553 (2014).

[10] Manjunatha N., Sumithra R. Effects of non-uniform temperature gradients on triple diffusive surface tension driven magneto convection in a composite layer. Universal Journal of Mechanical Engineering. **7** (6), 398–410 (2019).

[11] Awasthi M. K., Kumar V., Patel R. K. Onset of triply diffusive convection in a Maxwell fluid saturated porous layer with internal heat source. Ain Shams Engineering Journal. **9** (4), 1591–1600 (2018).

[12] Komala B., Sumithra R. Effects of non-uniform salinity gradients on the onset of double diffusive magneto–Marangoni convection in a composite layer. International Journal of Advanced Science and Technology. **28** (15), 874–885 (2019).

[13] Currie I. G. The effect of heating rate on the stability of stationary fluids. Journal of Fluid Mechanics. **29** (2), 337–347 (1967).

[14] Vidal A., Acrivos A. Nature of the neutral state in surface-tension driven convection. The Physics of Fluids. **9** (3), 615 (1966).

Потрійна дифузійна магнетоконвекція у рідинно-пористій композитній системі

Сумітра Р.[1], Комала Б.[2], Манджунатха Н.[3]

[1]*Кафедра UG, PG навчання та дослідження в математиці,*
Університет Нрупатунга, Бенгалуру, Карнатака, Індія
[2]*Кафедра природничих та гуманітарних наук, Університет PES,*
Бенгалуру, Карнатака, Індія
[3]*Факультет математики, Школа прикладних наук, Університет REVA,*
Бенгалуру, Карнатака, Індія

Досліджено потрійну дифузійну магнетоконвекцію для рідинно-пористої композитної системи з жорсткими межами, які ізольовані від температури та концентрації. Пористий шар композитної системи моделюється за допомогою моделі Дарсі–Брінкмана. Для визначення власного значення розглядуваної задачі використовується метод регулярних збурень. Критичне число Релея, яке є критерієм для початку конвекції, отримано для ступінчастої функції, засолювання нижче та знесолення вище профілів солоності. Графічно зображено вплив різних фізичних параметрів на початок конвекції та проаналізовано стійкість системи.

Ключові слова: *потрійна дифузійна магнетоконвекція; неоднорідні градієнти солоності; метод регулярных возмущений.*